



# Boosting dye-sensitized solar cell efficiency using AgVO<sub>3</sub>-doped TiO<sub>2</sub> active layer

Toka Hatem<sup>1</sup>, Maryam G. Elmahgary<sup>1</sup>, Rami Ghannam<sup>2</sup>, Mohamed A. Ahmed<sup>3</sup>, and Sameh O. Abdellatif<sup>4,\*</sup> 

<sup>1</sup>The Chemical Engineering Department, British University in Egypt (BUE), Cairo 11387, Egypt

<sup>2</sup>School of Engineering, University of Glasgow, Glasgow, UK

<sup>3</sup>Faculty of Science, Ain Shams University, Cairo, Egypt

<sup>4</sup>The Electrical Engineering Department, and FabLab, at the Centre of Emerging Learning Technologies CELT, British University in Egypt (BUE), Cairo 11387, Egypt

Received: 12 July 2021

Accepted: 6 September 2021

Published online:

14 September 2021

© The Author(s), under exclusive licence to Springer Science+Business Media, LLC, part of Springer Nature 2021

## ABSTRACT

Dye-sensitized solar cells have shown great potential in low and self-powered nano/micro-scale applications, due to their low fabrication costs, semi-transparency in the visible spectrum, diffused light harvesting capabilities, and their lead-free structure. However, DSSC efficiencies are still relatively low due to their limited absorption capabilities in the active mesoporous layer. The current study demonstrates an attempt to boost the overall conversion efficiency of DSSC by narrowing the energy band gap of the mesoporous TiO<sub>2</sub> active layer. AgVO<sub>3</sub> is utilized in doping the mesoporous layer, seeking for a visible absorption shift from 3.2 eV to 2.6 eV. In addition, natural organic beetroot dye is used while keeping DSSC with N719 dye as a bare cell. Morphological, optical, as well as electrical characterization results were obtained for both thin-film and complete solar cells. The fabricated cell showed an overall harvested power density of 8.6 mW/cm<sup>2</sup>, capable of operating various low-power sensing applications.

## 1 Introduction

TiO<sub>2</sub> films composed of nanoparticles in the range from 10 nm to 30 nm can have a roughness factor (the actual surface area to the apparent one) reaching 1000 [1]. Therefore, the amount of dye adsorbed in a DSSC is drastically increased due to the much larger accessible internal surface when the mesoporous TiO<sub>2</sub> is used. In fact, the space-filling capability of the

dye can reach almost 100% over a wide range in the visible region [1]. By virtue of comparison, the amount of adsorbed dyes on the surface of single-crystal and poly-crystal materials is quite small, causing only about 1% absorption even at the peak wavelength [1]. Such properties nominate mesoporous TiO<sub>2</sub> to be integrated in various optoelectronic applications [1–6]. One of these applications as

Address correspondence to E-mail: sameh.osama@bue.edu.eg

an active layer in dye-sensitized solar cells (DSSC) [6–8].

The absorption mechanism in the DSSC is mainly rely on the visible absorption due to the absorbed dye, as  $\text{TiO}_2$  is an UV absorber (3.2 eV) [4, 9]. Consequently, the reported DSSC efficiency is rarely reaching 10% [3, 10, 11]. Previous attempts in the literature acted to enhance the DSSC efficiency either by adding new trapping structures or by customizing the optical properties of the mesoporous  $\text{TiO}_2$  layer. In such context the  $\text{AgVO}_3$ -doped  $\text{TiO}_2$  thin film can be deposited using a simple sol–gel method [3]. Such doping can narrow down the energy band gap, turning mesoporous  $\text{TiO}_2$  to be a visible light absorber. Concerning the used dye, previous attempts were demonstrated with commercial N719 dyes. [1, 12, 13]. Alternatively, other attempts replaced the inorganic N719 dye with a low-cost organic dye based on beetroot. Organic beetroot dye recorded acceptable sustainability in previous attempts in the literature as well as matched optical spectrum with mesoporous  $\text{TiO}_2$  [14, 15].

The work investigated in this paper demonstrates the impact of  $\text{AgVO}_3$  doping on a mesoporous  $\text{TiO}_2$  layer used in organic-based dye-sensitized solar cells. Experimentally segmented and complete solar cells have been fabricated and characterized to evaluate the effect of doping on the overall conversion efficiency. The fabricated cell shoed acceptable output characteristics with  $8.6 \text{ mW/cm}^2$  harvested power density, as well as  $V_{oc}$  of 0.514 V and  $J_{sc}$  of  $20.9 \text{ mA/cm}^2$ . Herein, our fabricated cell can be used to harvest light for satisfying the energy demands of a

micro/nano-sensing unit. The low-power sensor was normally operated via the connected DC battery (cf. Fig. 1).

## 2 Experimental work and characterization

This section describes the fabrication process for a complete DSSC with organic dye and various  $\text{AgVO}_3$ -doping concentrations, applying a bottom-up approach. In addition, all morphological, optical, and electrical characterization procedures are explained.

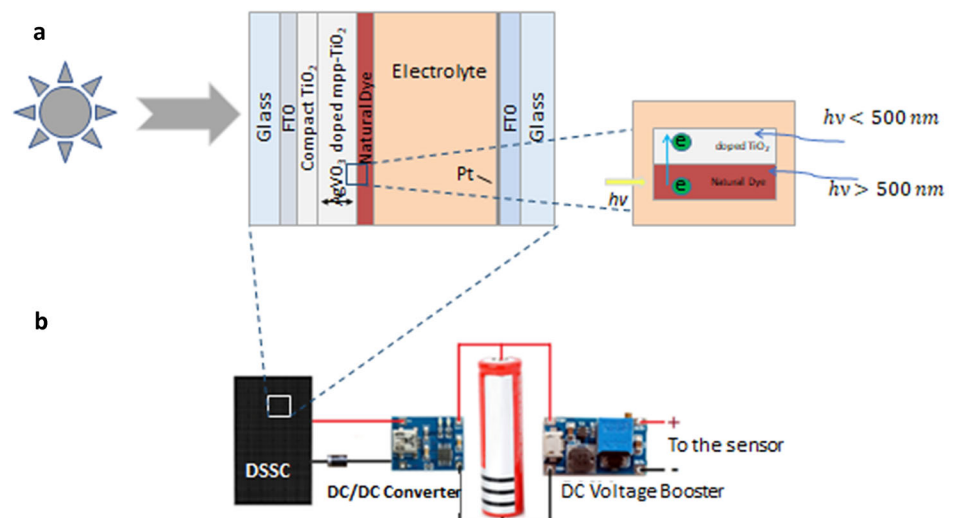
### 2.1 Materials

Titanium (IV) Iso-propoxide ( $\text{C}_{12}\text{H}_{28}\text{O}_4\text{Ti}$ , 97%), carboxy methyl cellulose sodium salt (CMC), and Iso-propyl alcohol ( $\text{C}_3\text{H}_8\text{O}$ ) were purchased from Sigma Aldrich for preparing  $\text{TiO}_2$  powder. Silver nitrate ( $\text{AgNO}_3$ ) and sodium vanadate ( $\text{NaVO}_3$ ) were purchased from Merck and used in preparation of the doped material. Acetonitrile ( $\text{CH}_3\text{CN}$ ), sodium hydroxide ( $\text{NaOH}$ ), ethylene glycol ( $\text{C}_2\text{H}_6\text{O}_2$ ), fluorescent dye, fluorine-doped tin oxide (FTO), iodine (I) G. R. grade, 99.8%, and potassium iodide (KI), were also purchased from Sigma Aldrich. N719 dye as well as natural dye, extracted from “Beet” and has a dark reddish-purple color, were used.

### 2.2 $\text{TiO}_2$ nanoparticles preparation and deposition

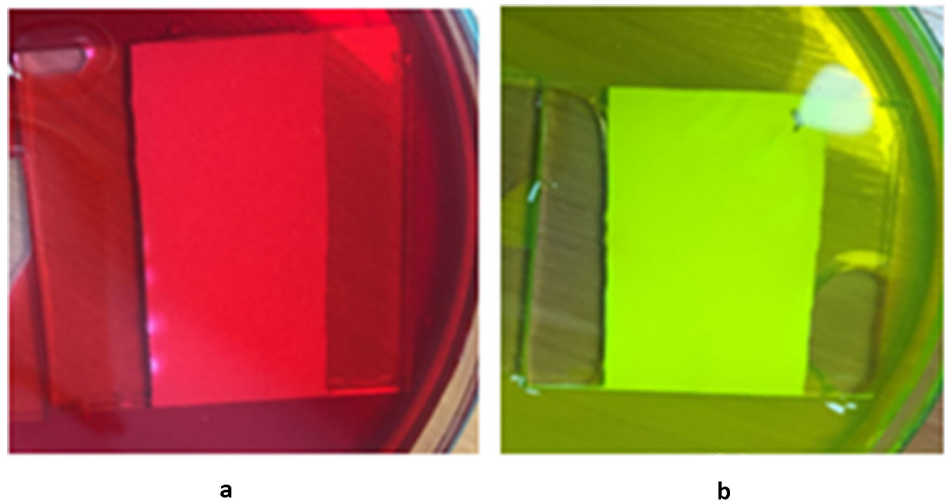
$\text{TiO}_2$  nanoparticles were prepared using the sol–gel method. 40 mL of titanium (IV) isopropoxide and

**Fig. 1** **a** Architecture of our DSSC **b** Diagram showing the location of the DSSC in our underwater light harvesting unit



**Table 1** Recipe and preparation of each layer for DSSCs

Step No	Step name	Needed chemicals and equipment	Description
1	Ethylene-glycol & Acetonitrile-based electrolyte	<ul style="list-style-type: none"> <li>• 0.24 g of I<sub>2</sub></li> <li>• 5 mL of Ethylene-glycol</li> <li>• 20 mL of Acetonitrile</li> <li>• 2.49 g of KI</li> </ul>	<ul style="list-style-type: none"> <li>• Add 0.24 g I<sub>2</sub> along with 2.49 g KI to 5 ml Ethylene-glycol</li> <li>• Add to the mixture 20 mL of Acetonitrile</li> </ul> Mix on magnetic stirrer for 30 min until the solution is homogenous
2	Triton-X based TiO <sub>2</sub> Paste for mesoporous layer	<ul style="list-style-type: none"> <li>• 2.5 g of TiO<sub>2</sub> powder</li> <li>• 3 mL Triton-X polymer</li> <li>• 0.75 ml iso-propanol</li> </ul>	<ul style="list-style-type: none"> <li>• Add 2.5 g of TiO<sub>2</sub> powder with 3 mL Triton-X polymer</li> <li>• Pestle till the mixture get homogenous</li> <li>• Using a micro-pipet add 0.75 ml of iso-propanol to the mixture and pestle again</li> </ul>
4	Compact TiO <sub>2</sub> layer	<ul style="list-style-type: none"> <li>• 170 mL of iso-propanol</li> <li>• 12 mL of titanium iso-propoxide</li> <li>• 0.4 mL of 2MHCL</li> </ul>	<ul style="list-style-type: none"> <li>• Add iso-propanol and titanium iso-propoxide while stirring</li> <li>• Drop by drop add 2 M of HCl</li> <li>• Stir using magnetic stirrer for over an hour</li> <li>• Store in a dark place</li> </ul>
5	Graphite on counter electrode	<ul style="list-style-type: none"> <li>• Graphite</li> </ul>	<ul style="list-style-type: none"> <li>• To prepare the counter electrode, a thin layer of graphite was traced on the FTO side of the counter electrode</li> </ul>

**Fig. 2** Thin layer of mp-TiO<sub>2</sub> immersed in **a** beet natural dye **b** N719 dye

400 mL of isopropyl alcohol (IPA) were mixed on a magnetic stirrer for 30 min at a speed of 100 rpm. Next, distilled water was added (drop by drop using a pipette) until a gel started to form. The solution was left for 2 days before it was later filtered, dried, grinded, and then calcinated for 3 h at 500 °C.

For paste preparation, 2.5 g of the prepared nanoparticles were added to 3 mL of CMC. The mixture was then grinded until it achieved the required homogeneity. Finally, 0.75 mL of IPA was

added to the mixture and grinded again. The film was screen printed on a glass substrate, as described in our previous work in [1, 12, 13].

### 2.3 Ag doing

Silver vanadate (AgVO<sub>3</sub>) was produced from the reacting sodium vanadate (NaVO<sub>3</sub>) and silver nitrate (AgNO<sub>3</sub>): “NaVO<sub>3</sub> + AgNO<sub>3</sub> → NaNO<sub>3</sub> + AgVO<sub>3</sub>.” NaVO<sub>3</sub> (1.5 mg) and AgNO<sub>3</sub> (2.09 mg) were placed

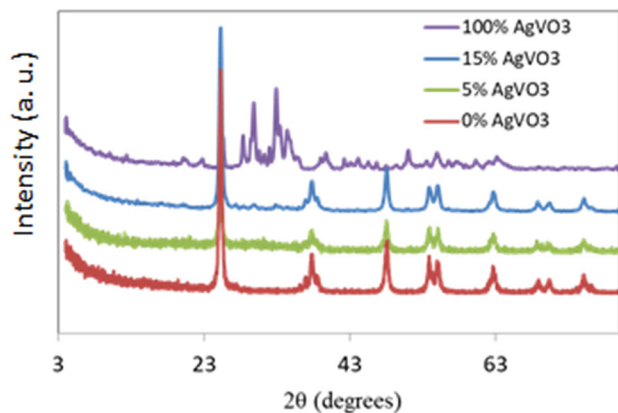


**Fig. 3** XRD patterns of  $\text{TiO}_2$ ,  $\text{TiAg}_5$ , and  $\text{TiAg}_{15}$ . The diffraction pattern of pure Titania shows several peaks at  $2\theta = 25.3^\circ$ ,  $36.9^\circ$ ,  $37.7^\circ$ ,  $38.5^\circ$ ,  $48^\circ$ ,  $51.9^\circ$ ,  $53.8^\circ$ ,  $55.1^\circ$ ,  $62.6^\circ$ ,  $68.7^\circ$ , and  $75^\circ$  [JCPDS No. 71–1167 were  $a = 3.786 \text{ \AA}$  and  $c = 9.507 \text{ \AA}$ ] referred to Titania anatase phase. These peaks were indexed in order of increasing diffraction angles indicated a body-centered tetragonal crystalline structure of Titania crystal

with 50 mL of distilled water on the magnetic stirrer until the crystals were completely dissolved in water and the solution was colorless. Next, the sodium vanadate solution was added drop by drop to the silver nitrate solution while stirring for 2 h, until it turned into a yellowish mustard color. Finally, after placing the mixture in a probe sonicator for 2 h, it was filtered, dried, and then grinded.

$\text{TiO}_2$  was doped with different concentrations of  $\text{AgVO}_3$ , varying from 0% to 25%. Powders were mixed in a beaker with 50 mL distilled water. Next, the mixture placed in a probe sonicator for 1.5 h and was again filtered, dried, and then grinded. Doped- $\text{TiO}_2$  pastes were then prepared using the same recipe mention in Sect. 2.2 and were deposited on glass using the screen-printing technique.

#### 2.4 Segmented and complete DSSCs fabrication

In comparison with our previously published work in [1, 12, 13, 16], we have replaced the commonly used N719 dye with an organic natural dye (detailed recipe is listed Table 1). Moreover, mp- $\text{TiO}_2$  was replaced by an  $\text{AgVO}_3$ -doped mp- $\text{TiO}_2$  layer, as discussed in the previous section. Herein, beetroot was used as a natural organic dye, which has a dark reddish purple color and has good sunlight absorption capabilities [6]. Beetroot-based dye was chosen due to its matched light spectrum, acceptable lifetime

as well as significantly reduced cost with respect to commercial N719 dye. For example, one gram of N719 approximately costs 330 euros, while the extracted organic dye costs less than 5% of this.

The extraction process was initiated by first rinsing the beetroot with water. They were later peeled and chopped to smaller parts. In a pan, distilled water was boiled with the chopped beetroot for around 15 min. After cooling down, the beetroot was squeezed using a hand blender until it turned into a paste. The observed consistency was very thick. A paper filter was then placed in a conical flask with a funnel. By adding pressure, the liquid beet natural dye was extracted, filtered, and ready for use.

Seeking for a bare cell, yellowish green N719 dye was prepared. The prepared concentration of the synthetic dye was  $2 \times 10^{-5}$  Molar. The medium is alkaline by using NaOH to increase the solubility of the dye in distilled water (see Fig. 2, green color in Fig. 2b is due to the  $\text{I}_3^-/\text{I}^-$  electrolyte). All DSSCs were sealed using a hot press at a temperature of  $120^\circ\text{C}$ .

#### 2.5 Characterization

The crystalline size and structure of the prepared nanoparticles were estimated by P Analytical X'PERT MPD diffractometer using  $\text{Cu [K}\alpha_1/\text{K}\alpha_2]$  radiation. The diffraction angle ranges from  $10^\circ$  to  $90^\circ$  with a step of  $0.02^\circ$  with integration time of three s/step were utilized. The morphologies of the samples were analyzed using high-resolution transmission electron microscopy (SEM JEOL 6340). To electrically characterize the fabricated DSSCs, an LED-based solar simulator with an integrated NIR-UV-Vis spectrometer and Keithley 2401 current-voltage source meter were used [17]. The optical transmission spectra of the fabricated as well as semifinished DSSCs are measured through a V-770 UV-Visible/NIR spectrophotometer that was used, which has a wavelength range from 190 nm to 2700 nm.

### 3 Results and Discussions

#### 3.1 $\text{TiO}_2$ nanoparticles characterizations

Following the  $\text{AgVO}_3$ -doped  $\text{TiO}_2$  nanoparticles recipe introduced in Sect. 2, XRD analysis was carried to investigate the crystal structure of the prepared



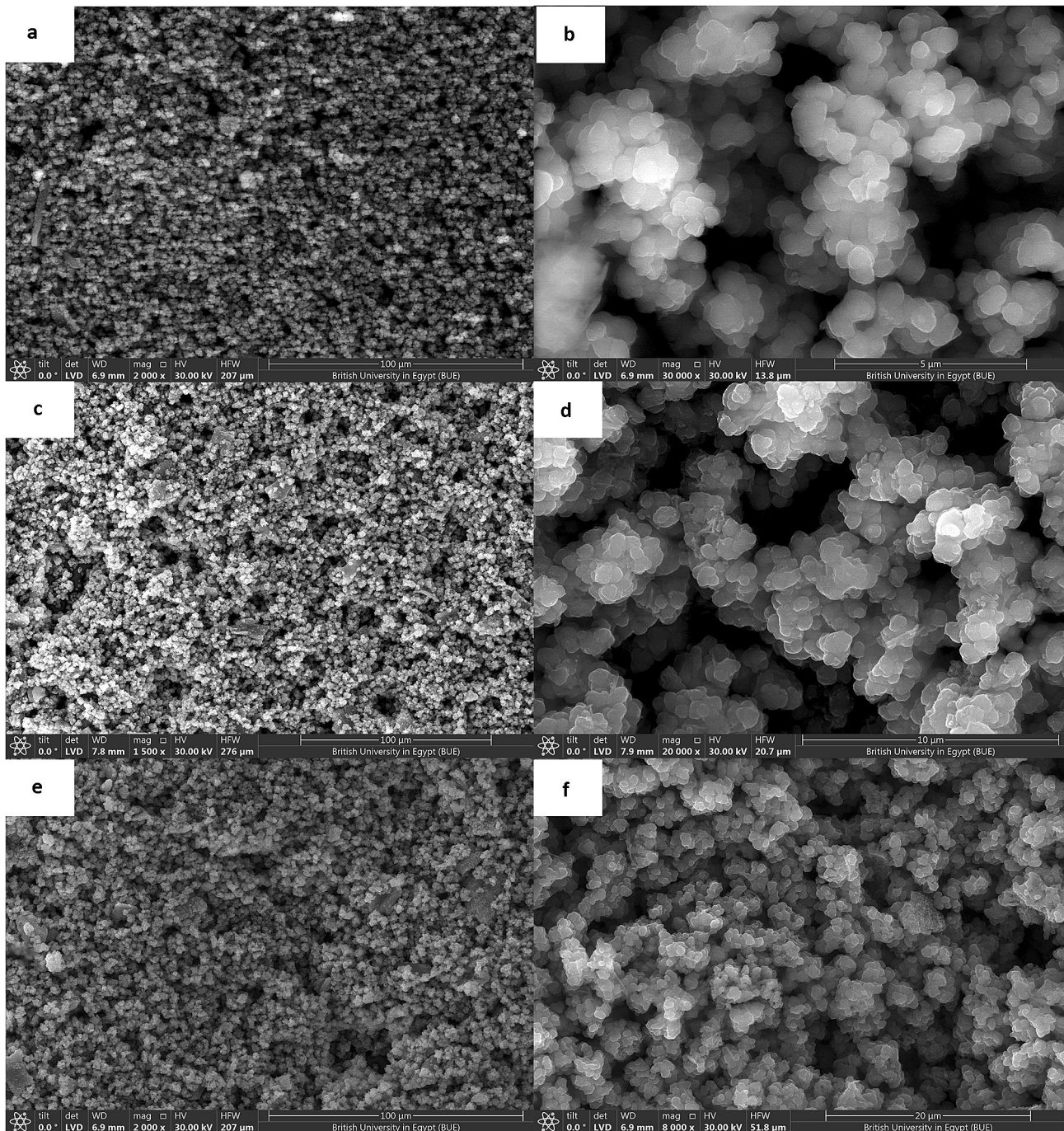


**Fig. 4** SEM for **a** and **b**  $\text{TiO}_2$ , **c** and **d**  $\text{TiO}_2$  doped with 5%  $\text{AgVO}_3$ , and **e** and **f**  $\text{TiO}_2$  doped with 15%  $\text{AgVO}_3$

nanoparticles. XRD was conducted for  $\text{TiO}_2$ ,  $\text{AgVO}_3$ ,  $\text{TiO}_2$  doped with 5% to 25% to ensure that the required structures were formed. Figure 3 shows the XRD patterns of  $\text{TiO}_2$ ,  $\text{TiAg}_5$ , and  $\text{TiAg}_{15}$ . The XRD pattern of the nanocomposite shows the existence of broad peak revealing the reduction in Titania crystallites upon incorporation of bismuth vanadate. The diffraction pattern of pure Titania shows several

peaks at  $2\theta = 25.3^\circ, 36.9^\circ, 37.7^\circ, 38.5^\circ, 48^\circ, 51.9^\circ, 53.8^\circ, 55.1^\circ, 62.6^\circ, 68.7^\circ, \text{ and } 75^\circ$  [JCPDS No. 71-1167 were  $a = 3.786 \text{ \AA}$  and  $c = 9.507 \text{ \AA}$ ] referred to Titania anatase phase. These peaks were indexed in order of increasing diffraction angles indicated a body-centered tetragonal crystalline structure of Titania crystal. The XRD pattern of the nanocomposite shows the existence of broad peak revealing the reduction in

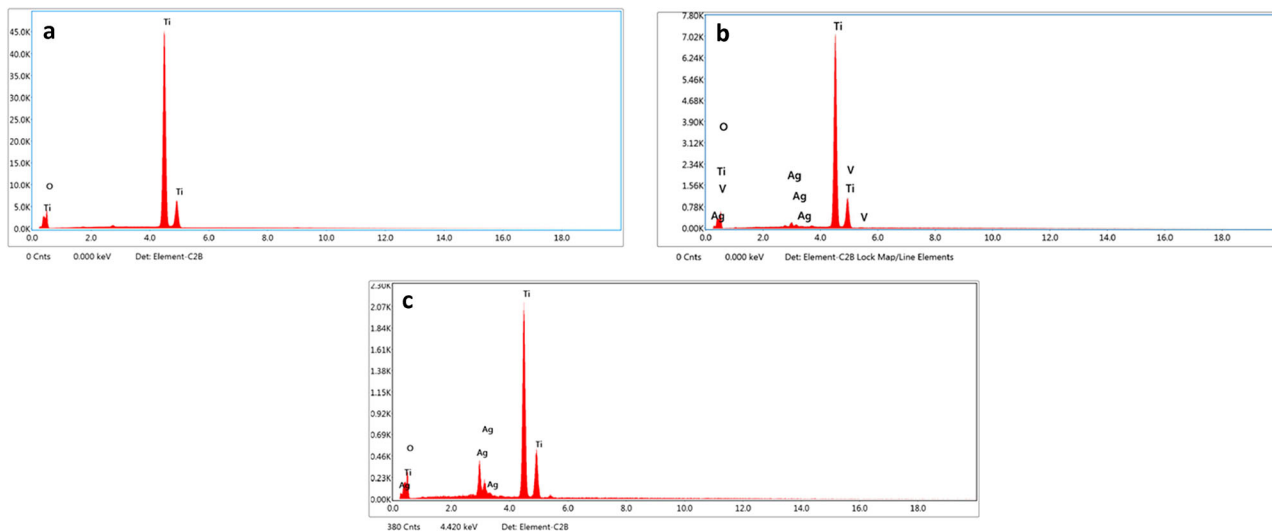


Fig. 5 EDX for a  $\text{TiO}_2$  b  $\text{TiO}_2$  doped with 5%  $\text{AgVO}_3$ , and c  $\text{TiO}_2$  doped with 15%  $\text{AgVO}_3$

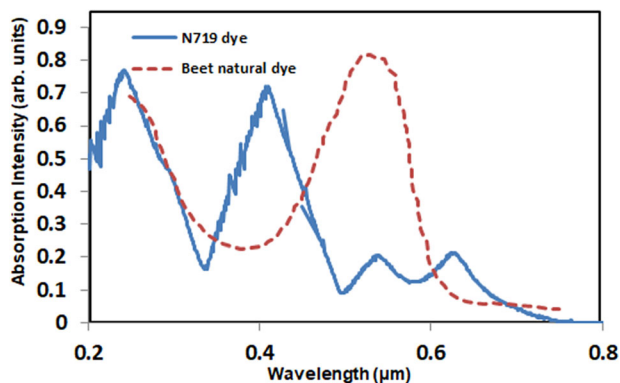


Fig. 6 Absorption spectra for a N719 and b Beetroot dye

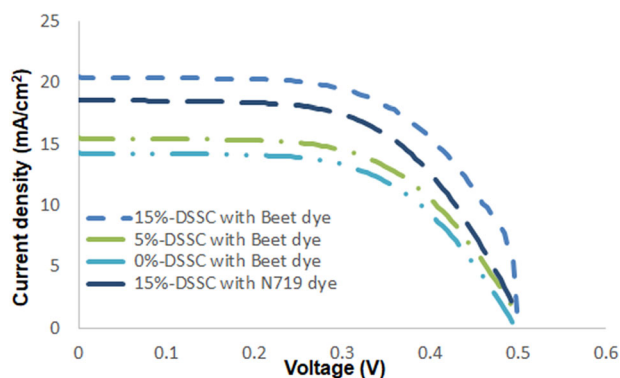


Fig. 7 J-V characteristic curves for fabricated DSSCs with N719 dye and beetroot dye associated with variable doping level of  $\text{AgVO}_3$  in the mesoporous active layer

Titania crystallites upon incorporation of bismuth vanadate. This result reflects the strong chemical

interaction between  $\text{AgVO}_3$  and anatase  $\text{TiO}_2$  to form titanium vanadium hydroxide.

### 3.2 $\text{TiO}_2$ thin-film characterizations

Using the recipe discussed in Sect. 2,  $\text{TiO}_2$  paste was deposited on microscopic glass substrates. Three sets of samples were prepared using  $\text{TiO}_2$  paste as well as  $\text{AgVO}_3$  doped. SEM characterization analysis is carried out for the deposited thin layer to determine the surface characteristics, size and shape of particles, composition, and arrangement of atoms in the sample. Measurements were conducted for  $\text{TiO}_2$  and  $\text{TiO}_2$  doped with 5% to 25%. As shown in Fig. 4, the anatase titanium dioxide mesoporous layer which is prepared by sol-gel method [1, 12] has a homogeneous structure and is highly crystalline with spherical agglomerated particles.

EDX characterization analysis is attached in Fig. 5. EDX characterization analysis is carried out to determine and identify the elements present in the sample with information about their percentages (see Fig. 5). Analyses illustrate the elements presented in  $\text{TiO}_2$  are Ti and O, while the elements presented in  $\text{TiO}_2$  doped 5% and 15% are Ti, O, Ag, and V, with the indicated percentages in the graphs (c.f. Fig. 5b and c).

### 3.3 Optical characterizations

We compared the absorption spectrum of beetroot dye standard N719 dye (see Fig. 6). For the N719



**Table 2** J-V characteristic outputs for fabricated DSSCs with N719 dye and Beetroot dye associated with variable doping level of AgVO<sub>3</sub> in the mesoporous active layer. Comparison is made with previous reported data in [13, 15, 19]

Cell type	$V_{OC}$ (V)	$J_{SC}$ (mA/cm <sup>2</sup> )	FF	$V_m$ (V)	$J_m$ (mA/cm <sup>2</sup> )	Efficiency (%)
0% with beet dye (bare cell)	0.502	13.8	0.78	0.416	12.8	5.3
5% with beet dye	0.513	15.3	0.77	0.426	14.1	5.9
15% with N719 dye	0.533	18.7	0.79	0.447	17.4	7.8
15% with beet dye	0.514	20.9	0.81	0.445	19.8	8.6
Bare DSSC-A in [13]	0.615	1.2	0.61	0.498	1.08	2.18
Red turnip-based DSSC in [15]	0.425	9.5	0.37	Not given	Not given	1.7
Doped 1Cu/TiO <sub>2</sub> with N719 dye as reported in [19]	1.073	7.3	0.65	Not given	Not given	5.1

commercial dye, double absorption peaks were recorded (at 289 nm and 456 nm), which agrees with previous reported data in the literature in [18]. The variation in the wavelength allocation of the two detected peaks in the N719 spectrum as well as the spectrum sharpness can be attributed to the dye treatment method along with the dilution percentages. It can be observed that the natural beetroot dye, with peak absorption around 550 nm (centralized visible absorption spectrum), is more appropriate for the proposed DSSC compared with N719 dye. This is due to the enhanced absorption of the doped TiO<sub>2</sub> layer, making it capable of absorbing near ultra-violet photons in the visible portion of the spectrum (350 nm to 500 nm). Accordingly, the integration of the AgVO<sub>3</sub>-doped TiO<sub>2</sub> layer with the beetroot natural dye will broaden the absorption spectrum of the effective active layer in DSSC.

### 3.4 Electrical characterizations

The J–V characteristic curves for the fabricated DSSCs are shown in Fig. 7. In the current study, we investigated the impact of both AgVO<sub>3</sub> doping as well as the beetroot dye. First, it can be observed that the higher the doping rate, the higher the short-circuit current density. Maximum is obtained when the doping rate reached 15% with current density of 20.9 mA/cm<sup>2</sup>. This condition represents the maximum efficiency of around 8.6% with total extracted power density around 8.6 mW/cm<sup>2</sup>. Consequently, by referring to the bare cell with N719 dye, still the beetroot dye recorded higher current as well as efficiency with respect to N719 DSSC. Beetroot dye showed an enhanced performance by nearly 10% while considering N719 dye as a reference keeping the doping level constant in both as 15% (cf. Fig. 7).

This agrees with the interpretation proposed earlier related to the matching in the spectra between organic beetroot dye and the mesoporous TiO<sub>2</sub> layer with narrowed energy band gap. Herein, a merged absorption profile with visible absorption overlapping is resulted, which can maximize the absorption in the active layer. Accordingly, we can describe the proposed DSSC as a double absorption effect DSSC, where both the AgVO<sub>3</sub>-doped TiO<sub>2</sub> and the dye are contributing to the absorption mechanism. All output characteristic parameters are listed in Table 2.

By referring to the literature, we can figure out that the measured efficiency with 15% doping and beetroot dye enhanced the efficiency of the proposed DSSC from 2.1% (see reported efficiency in [13], under DSSC-A samples) to nearly 8.6%. Other literature attempts recorded higher references [15, 19]; however, the reported efficiencies were still below 8.6%, see Table 2. Our proposed cell can be categorized as a very low cost, simple, and low-temperature fabricated cell. Such conservations promoted organic dye-based DSSCs in various micro/nanopower applications. Finally, the sustainability performance analysis of these devices needs to be investigated in the future.

## 4 Conclusion

This work presents a boosted 6.1% DSSC through narrowing the energy band gap of the active mesoporous TiO<sub>2</sub> layer as well as integrating a natural dye. Mesoporous TiO<sub>2</sub> is treated with 15% of AgVO<sub>3</sub> to reach an energy band gap of 2.6 eV. The optimized cell with energy harvesting density of 8.6 mW/cm<sup>2</sup> was recorded. The proposed cell showed enhanced performance with respect to a bare cell fabricated

with N719 dye as well as similar recipes reported data in the literature. The harvested output power is capable of operating various IoT low-power applications towards a self-power sensor.

## Acknowledgements

The authors would like to acknowledge the support and contribution of the STDF in this work. As part of the STDF Project entitled, “Mesostructured Based Solar Cells for Smart Building Applications,” Project ID#33502.

## Author contributions

All authors have contributed equally.

## Funding

The authors would like to acknowledge the support and contribution of the STDF in this work. As part of the STDF Project ID#33502.

## Data availability

The data that support the findings of this study are available as following: <https://www.mathworks.com/matlabcentral/fileexchange/76474-dssc-optical-modelling>. Any other data that support the findings of this study are available from the corresponding author upon reasonable request.

## Code availability

Not applicable for that section.

## Declarations

**Conflict of interest** The authors declare that there is no conflict of interest.

**Ethical approval** Not applicable for that section.

**Consent to participate** All authors confirm the participation in this paper.

**Consent for publication** All authors accept the publication rules applied by the journal.

## References

1. S. Abdellatif, S. Josten, P. Sharifi et al., Physics and Simulation of Optoelectronic Devices XXVII International Society for Optics and Photonics. 1991 Nature **353**, 737 (2018)
2. C-W Luo, AP Thilakan, J-X Li, et al. (2020) UV degradation mechanism of TiO<sub>2</sub>-based perovskite solar cells studied by pump-probe spectroscopy. SPIE
3. D. Dey, N. Halder, K.P. Misra, S. Chattopadhyay, S.K. Jain, P. Bera, N. Kumar, A.K. Mukhopadhyay, Systematic study on the effect of Ag doping in shaping the magnetic properties of sol-gel derived TiO<sub>2</sub> nanoparticles. Ceram. Int. **46**(17), 27832–27848 (2020). <https://doi.org/10.1016/j.ceramint.2020.07.282>
4. T.A. Egerton, N.J. Everall, J.A. Mattinson, L.M. Kessell, I.R. Tooley, J. Photochem. Photobiol., A **193**, 10 (2008)
5. Y. Zhang, G. Li, Y. Wu, Y. Luo, L. Zhang, J. Phys. Chem. B **109**, 5478 (2005)
6. S. Sathyajothi, R. Jayavel, A.C. Dhanemozhi, Materials Today: Proceedings **4**, 668 (2017)
7. K.H. Ko, Y.C. Lee, Y.J. Jung, J. Colloid Interface Sci. **283**, 482 (2005)
8. G. Deogratias, N. Seriani, T. Pogrebnaya, A. Pogrebnoi, J Mol Graph Model **94**, 107480 (2020)
9. C-W Luo, AP Thilakan, J-X Li, et al. (2020) Photonics for solar energy systems VIII International society for optics and photonics
10. M.A. Liaqat, Z. Hussain, Z. Khan, M.A. Akram, A. Shuja, Effects of Ag doping on compact TiO<sub>2</sub> thin films synthesized via one-step sol-gel route and deposited by spin coating technique. J. Mater. Sci.: Mater. Electron. **31**, 7172–7181 (2020)
11. E.M. Hashem, M.A. Hamza, A.N. El-Shazly, M.F. Sanad, M.M. Hassan, S.O. Abdellatif, Nanotechnology **32**, 085701 (2020). <https://doi.org/10.1088/1361-6528/abca29>
12. S. Abdellatif, P. Sharifi, K. Kirah et al., Microporous Mesoporous Mater. **264**, 84 (2018)
13. S.O. Abdellatif, S. Josten, A.S. Khalil, D. Erni, F. Marlow, IEEE J Photovolt **10**, 522 (2020)
14. R. Grisorio, L. De Marco, C. Baldisserri et al., ACS Sustain Chem Eng **3**, 770 (2015)
15. S. Shalini, R. Balasundaraprabhu, T.S. Kumar, N. Prabavathy, S. Senthilarasu, S. Prasanna, Int. J. Energy Res. **40**, 1303 (2016)
16. AKM Mohamed O. Ahmed, Peter Makeen, Shehab Edin I. Betelmal, Minatallah M. Hassan, Mohamed M. Abdelsamee,



- Ahmed Ayman, Mohamad H. El-Adly, Ashraf Nessim, Sameh O. Abdullatif (2021) WSEAS Transact Environ Dev 17: 118. <https://doi.org/10.37394/232015.2021.17.12>
17. MM Hassan, A Sahbel, SO Abdellatif, KA Kirah, HA Ghali (2020) New concepts in solar and thermal radiation conversion III International society for optics and photonics
  18. M. Hočevar, U. Opara Krašovec, M. Berginc, M. Topič, One step preparation of TiO<sub>2</sub> layer for high efficiency dye-sensitized solar cell. Acta Chim. Slov. 57, 405–409 (2010)
  19. B. Ünlü, M. Özacar, Sol. Energy 196, 448 (2020)

**Publisher's Note** Springer Nature remains neutral with regard to jurisdictional claims in published maps and institutional affiliations.